INSTITUTE OF PLASMA PHYSICS

NAGOYA UNIVERSITY

RESEARCH REPORT

NAGOYA, JAPAN

Ion Cyclotron Heating of a Plasma and Energy Confinement in a Toroidal Quadrupole

T. Takizuka*, H. Abe*, H. Momota*
and C. Namba

IPPJ-200 September 1974

Further communication about this report is to be sent to the Research Information Center, Institute of Plasma Physics, Nagoya University, Nagoya, Japan.

---

* Permanent address : Faculty of Engineering, Kyoto University, Kyoto

Abstract

With the use of rf electric fields, the heating of the plasma and the improvement in the energy confinement are studied for an open-ended toroidal quadrupole. After analyzing loss mechanisms of the plasma and the heating rate, both theoretically and numerically, some optimizations have been made. The resultant heating and energy confinement are exhibited in the computer experiments. The plasma can be heated easily and the improvement in the energy containment time ~ 10 % is obtained.

§1. Introduction

Among the magnetic confinement systems of plasmas, the open systems have been emphasized to have several advantages over the closed ones. There is, however, an essential disadvantage inherited to the open systems, that is, their large end loss. In these situations, a number of trials have been made in order to improve the energy confinement in an open system. Applications of rf electromagnetic fields on open-ended plasmas have also been investigated[1-3] for the purpose of the improvement in energy confinements, besides the heating of plasmas. In an open-ended toroidal quadrupole, a possibility of the improvement in the energy confinement by means of the applied electric field with the ion cyclotron frequency has been pointed out by Abe et al[4]. They have carried out the computer experiment based on the "Collisionless PIC method". In their treatment, however, the rf electric field has been applied in a simplified way, and collisions have been introduced only for ions on the basis of a model of large angle scattering.

In this paper, the model for computer experiments succeeds mainly to the above paper. The design of the device is illustrated in Fig.1. The rf electric field is applied through the electrodes, and collisional effects are introduced both for ions and electrons. Further, a collision model is introduced by utilizing a modification of Langevin's equation so as to include the small angle scatterings.

In the subsequent section (Sec.2), we shall study loss

mechanisms of the contained plasma energy in the toroidal quadrupole. The classical mirror loss, the mirror loss due to the nonadiabatic motion of a charged particle, and the "banana" diffusion which originates from the toroidality of the system and is essentially the same as in Tokamaks, are discussed. Effects of the rf electric field on the heating and the confinement of the plasma are investigated in Sec.3. Since the energy of the particle contained in a container is limited, a kind of feedback control is required. This is discussed in Sec.4. In order to check these results, various numerical studies have been carried out in a single particle model. An optimization of parameters has been made. Complete computer experiments are described in Sec.5. An effective heating of the plasma is observed, as well as an improvement in the energy confinement to a certain extent. Section 6 is devoted to conclusions and discussions.

§2. Loss mechanisms

A plasma in a toroidal quadrupole without an external rf electromagnetic field may be lost due to (i) the classical mirror loss, (ii) the mirror loss caused by the variation of the magnetic moment at the region where the curvature of the magnetic line of force is large, and (iii) the enhanced diffusion attributed to the "banana motion". Because of our model, anomalous losses caused by instabilities are not taken into account.

(i) *Classical mirror loss*

We shall begin our discussions by assuming that the particle loss in a magnetic mirror is essentially ruled by the ion loss.

Consider an ion trapped in the magnetic mirror. It should initially have a velocity vector pointing outside the loss cone, but after some encounters with other particles its velocity may eventually be put into the loss cone and it will be lost through an open end of the mirror. The collisional change of the velocity is naturally not one way, but it is quite often that an ion tentatively belonging to the loss cone may recover the trapped condition after collisions. The latter process is important when the ion collision time τ_{ic} is not so large compared with its transit time τ_{it} between mirrors, and this is fully taken into account in the present computer analysis. In these situations, the containment time of a charged particle τ_n is obtained as (Appendix A)

$$\tau_n \simeq \tau_{ic} \ln R_m + 2R_m \langle \tau_{it} \rangle \quad , \tag{2.1}$$

where $\langle \tau_{it} \rangle$ is the mean transit time of ions. The mirror ratio R_m of the toroidal quadrupole is defined by

$$R_m = \frac{B(x=a, y=a)}{(x=0, y=0)} \simeq \frac{\sqrt{2+\gamma^2}}{\gamma} \quad , \tag{2.2}$$

where γ denotes the ratio of the toroidal magnetic field B_t to the cusped magnetic field B_c.

(ii) *Mirror loss due to the nonadiabatic nature*

The magnetic moment of a charged particle can be defined to be $\mu = Mv_{\perp}^2/2B$ in the adiabatic region in which an adiabatic parameter A is large enough. In such a region this quantity is well conserved along the particle path, if collisions are absent. Here, the adiabatic parameter is defined as the ratio r_c/r_L, where r_c denotes the radius of curvature of a line of force and r_L is the gyration radius. In the toroidal quadrupole whose cross section is a square with side $2a$, the adiabatic parameter along the line $y=x$ or $y=-x$ is explicitly written in terms of the quantity r_{L0}, the gyration radius defined by the cusped magnetic field, as

$$A = \frac{r_c}{r_L} \simeq \frac{a}{r_{L0}} \frac{1}{\gamma} \frac{a}{\sqrt{x^2+y^2}} \left(\frac{x^2+y^2}{a^2} + \gamma^2\right)^2 . \tag{2.3}$$

The value of A is illustrated in Fig.2 as a function of $\sqrt{x^2+y^2}$. The minimum of the adiabatic parameter is approximately

$3\gamma^2 a/r_{L0}$ at the point $\sqrt{x^2+y^2} = \gamma a/\sqrt{3}$.

The magnetic moment cannot preserve its original value across the region where A is small. The relative change of the magnetic moment is considered[5] proportional to $\exp(-A)$. Accordingly, the mirror ratio of the toroidal quadrupole becomes large, then the variation of the magnetic moment of a charged particle also becomes large. The change in the magnetic moment obviously causes the loss of the plasma even when collisions are absent. For a typical case that R_m is 14 and the minimum of the adiabatic parameter of an ion $A_{i|min}$ is nearly 1.5, the trajectory of an ion and the time variation of the quantity μ are illustrated in Figs.3(a) and (b), where the ion escapes finally to an open end.

On the other hand, if the adiabatic parameter is not so small, then the following occures in the collisionless plasma. Even if the quantity μ varies in the nonadiabatic region, the magnetic moment recovers the previous value after the passage through the nonadiabatic region. This behaviour is typically shown in Fig.4(a), where $A_{i|min}$ is about 8. It must be noted that the particle is not lost in this case. However, as is seen in Fig.4(b), the presence of rare collisions makes the magnetic moment change by the order of the variation of μ in the nonadiabatic region. Therefore the loss of the plasma is enhanced compared with that indicated by Eq.(2.1).

Figure 5 demonstrates the decay of the particle number in three runs of the simulation, where the values of the mirror ratio are chosen to $3, 5$, and 14. Other physical

quantities are listed up on Table I. In the first case where R_m is 3 and the mean of $A_{i|min}$ is 40, the particle containment time is observed to be about 50 μsec, which is quite comparable with the classical value (50 μsec) given by Eq.(2.1). On the other hand, in the second case, when R_m=5 and the mean of $A_{i|min}$ is 13, the containment time is rather small compared with the classical one. In the third case that R_m is as large as 14 and the mean of $A_{i|min}$ is 1.5, the number of ions remaining in the container decreases much more rapidly.

(iii) *Enhanced cross field diffusion*

Consider a case where collisions are absent and the magnetic moment is conserved in a toroidal quadrupole, the motion of some guiding center forms a "banana" orbit, as is illustrated in Fig.6. The largest width of this "banana" orbit δr is given approximately by (Appendix B)

$$\delta r \simeq \sqrt{2}\, r_L \sqrt{a/r_L} \quad \text{for} \quad r_L << \gamma^2 a$$

and (2.4)

$$\delta r \simeq \sqrt{2}\, \gamma\, a \quad \text{for} \quad r_L >> \gamma^2 a.$$

Note that δr is much larger than the gyration radius, and consequently the cross field diffusion is enhanced because of its large step length. Therefore, ions are lost into rf electrodes through this cross field diffusion, even if the gyration radius is much smaller than the interval of the electrodes. Table II shows the relative number and the mean energy of those ions lost into rf electrodes, which

are observed in simulation runs.

Accordingly, we assume the rf electrodes of ideal mesh type, hereafter, so that high energy ions may not be lost into them.

§3. Effects of the rf electric field on the heating and the confinement

It is well known[6] that ions may be heated by applying an rf electric field in the vicinity of ion cyclotron angular frequency ω_r. However, it is not obvious[7-9] whether the rf electric field can effectively decrease the loss of the plasma in an open system.

Heating rate

The change of an ion energy for a passage through the resonance zone has been given by Kawamura et al[10]. In our notations, it takes the form

$$\Delta W = \sqrt{W_{\perp 0}/2M}\; eE_0 t_r \cos\phi + (e^2/2M) E_0^2 t_r^2 \,, \tag{3.1}$$

where $W_{\perp 0}$ is the transeverse energy before entering the resonance zone, E_0 is the amplitude of the applied rf electric field, ϕ is the initial phase difference between the gyration and the rf electric field, and t_r is the effective duration through the resonance zone.

If the gyration phase is random at each passage through the resonance zone, then the heating rate is roughly given by

$$\frac{d\langle W_i \rangle}{dt} \simeq \alpha\, E^2{}_0 \tag{3.2}$$

and

$$\alpha \simeq 5 \times (e^2/M)(\delta N/N)\omega_r^{-1} \,, \tag{3.3}$$

where $\langle W_i \rangle$ is the mean ion kinetic energy, δN is the number

of ions which pass through the resonance zone, and N is the total number of ions. A comparison of Eq.(3.2) with the results of simulation runs is made in Fig.7, where the value of ω_r is $4.5 \times 10^7 \mathrm{sec}^{-1}$ and the resultant value of $\alpha \simeq 0.8$ $\mathrm{eV \cdot sec^{-1} \times (V/m)^{-2}}$ agrees with that calculated from Eq.(3.3). The ratio $\delta N/N$ is assumed to be about 10 %.

Effect on the confinement

By applying the rf electric field, an ion in the loss cone may be put into the trapped region, if its magnetic moment is increased by a certain amount. Putting the second term on the rhs of Eq.(3.1) to be larger than the first term (except for the factor cos ϕ), one can express the above condition as

$$E_0^2 \gtrsim (\sqrt{M}\ \omega_r / ae^2)\sqrt{W_{ir} W_{i\perp}} \quad , \tag{3.4}$$

where W_r stands for the parallel kinetic energy at the resonance zone.

On the other hand, if the second term is much smaller than the first one, the rf electric field cannot reduce the classical mirror loss. In addition, some ions in the trapped region may fall into the loss cone, because their magnetic moments are decreased by the rf electric field. In this case, the resultant loss rate is increased in comparison with the classical mirror loss.

Consider the case that condition (3.4) is initially

satisfied for all ions. After a number of passages through the resonance zone, some ions are accelerated and accordingly the condition breaks down for these ions. And as a result, the loss rate of ions may increase gradually. This situation is seen in a simulation run which is presented in Fig.8. In this case, E_0 is set as *20* kV/m. Ions with an initial temperature of *300* eV are completely contained at the initial stage, where the lhs of condition (3.4) is larger than three times of the rhs. After a few bounces of ions, (*10* μsec), however, the mean kinetic energy of ions is increased and condition (3.4) is no more satisfied for some ions, i.e., the rhs becomes comparable to the lhs. At this time, the loss rate of ions is larger compared with the classical mirror loss.

§4. Feedback control of rf electric fields

As is shown previously, if the energy of a particle is above a certain value, the applied rf electric field has no effect on the improvement in the particle confinement in an open system. Accordingly, it is necessary for suppressing plasma losses that the amplitude E_0 is changed in accordance with the kinetic energy of ions.

Feedback control

If condition (3.4) is always satisfied for the majority of ions, then the plasma loss may be suppressed. Therefore we shall introduce the amplitude E_0 increasing in proportional to the mean kinetic energy of ions:

$$E_0^2 = C\langle W_i \rangle \quad . \tag{4.1}$$

Condition (3.4) is fulfilled as for ions whose kinetic energy $W_i \lesssim \langle W_i \rangle$ by setting $C \sim \sqrt{MW_{ir}}\ \omega_r/ae^2$, and then these ions do not escape from the container. However, the loss of high energy ions cannot be suppressed completely by this method. We have evaluated the effect of the rf electric field by measuring the energy containment time τ_E. The values of the energy containment time of the ion component obtained in simulation runs are plotted in Fig.9 as a function of the constant C, where ω_r is 6.8×10^7 $\sec^{-1}$, a is 0.25m, and W_{ir} is about 10 eV. This figure shows a peak around $C = 1.5 \times 10^5$ $(\mathrm{V/m})^2/\mathrm{eV}$. This value may be compared

with 10^5 (V/m)^2/eV which is estimated from condition (3.4). In Fig.10, the typical data ($C = 1.5 \times 10^5$ (V/m)^2/eV) of the contained ions, the contained ion energy, and the lost ion energy are shown, and the data without the rf electric field are also given for comparison.

If the value of C is too large, ions are ready to be separated into two groups; one consists of a few high energy ions and the other consists of the majority of ions with low energy. Condition (3.4) is no more satisfied for ions belonging to the former group. This corresponds to the gradual decrease of τ_E for larger C in Fig.9.

Heating rate

The heating rate of ions in the feedback system introduced here is derived from Eqs.(3.2) and (4.1) in the form;

$$\frac{d\langle W_i \rangle}{dt} \simeq \frac{1}{\tau_H} \langle W_i \rangle \ , \qquad (4.2)$$

where the heating rate τ_H^{-1} equals to αC. The evolution of the mean ion energy which is obtained in a simulation run is illustrated in Fig.11. The value of ω_r is 6.8×10^7 sec^{-1} and C is chosen as 2.5×10^5 (V/m)^2/eV. The heating rate $\tau_H^{-1} \simeq 1.4 \times 10^5$ sec^{-1} obtained in this figure agrees with 1.3×10^5 sec^{-1} calculated from Eq.(4.2).

§5. Computer experiments

Parameters employed in the complete computer experiments are chosen on the basis of the above studies, and are listed in Table III. The mirror ratio is settled to be *3* so that the adiabatic parameter is large enough. The feedback system is performed by choosing $C = 1.5 \times 10^5 (\mathrm{V/m})^2/\mathrm{eV}$, and the quantities for the computations are chosen as shown in Table IV.

In order to avoid effects which may be brought about by an initialization[4] of the charged particle system, the rf electric field is not applied for the first *3* μsec, and then it is applied until the time $t = 18$ μsec (Experiment I). For comparison of the results, other computer experiments have been carried out for two cases: in Experiment II, the rf electric field is absent over the experiment, and in Experiment III, the rf electric field is turned off at the time $t = 12$ μsec.

The improvement in the particle containment time is seen in Fig.12. Between the time $t = 3$ μsec and $t = 12$ μsec, the particle containment time in Experiment II is $\tau_{nII} =$ 35 μsec, while in Experiment I the rf electric field increase τ_{nI} to be *39* μsec. Similarly, between the time $t = 12$ μsec and $t = 18$ μsec, $\tau_{nI} = 35$ μsec should be compared with the containment time in Experiment III, i.e., $\tau_{nIII} = 31$ μsec. The values τ_{nII} and τ_{nIII} obtained in the computer experiments are coincide with the value calculated from Eq.(2.1), provided that the mirror ratio R_m is replaced by the effective one[11]:

$$R_{m\ eff} = R_m/(1 + e\phi/\langle W_i \rangle) , \qquad (5.1)$$

where ϕ represents the mean plasma potential. The spatial distributions of the plasma potential in Experiment II and I at the time $t = 9$ μsec are illustrated in Figs.13(a) and (b), respectively.

The evolution of the contained energy of the plasma and that of the lost energy are demonstrated in Fig.14, where the contained energy consists of the kinetic energy and the potential energy of ions as well as electrons.

As well as the particle confinement, a careful application of the rf electric field brings about a certain improvement in the energy confinement. In fact, the energy containment time τ_{EI} is 47 μsec for the first 9 μsec or is 41 μsec for the last 6 μsec, in Experiment I. These values must be compared with $\tau_{EII} = 43$μsec (Experiment II) or $\tau_{EIII} = 37$ μsec (Experiment III), respectively. Therefore, in this case, the rf electric field improves the energy confinement about 10 %.

The rf electric field may raise the ion energy. As is shown in Fig.15(a), the mean ion energy increases by a factor 3 for the time interval of 15μsec. The heating rate $\tau_H^{-1} = 8.3 \times 10^4$ sec^{-1} observed in this experiment agrees with that calculated from Eq.(4.2). On the contrary the electron temperature is not affaired by the rf electric field as is shown in Fig.15(b).

§6. Conclusions and discussion

We have first studied loss mechanisms of the energy of the plasma contained in a toroidal quadrupole. If the mirror ratio is small, the classical mirror loss and the banana diffusion are appreciable. On the contrary, if the mirror ratio is large, then the nonadiabatic motion of a charged particle enhances the particle loss. In our computer experiments, the mirror ratio $R_m = 3$ has been employed.

Effects of the applied rf electric field have been considered. The heating rate by the rf electric field is descrived by Eq.(3.2). In order to obtain a good confinement of the plasma, some feedback control of the rf electric field must be required. According to the simplified simulation, a certain optimized feedback system is introduced.

Computer experiments have been carried out with optimized parameters in the toroidal quadrupole. The plasma has been heated easily and the improvement in the energy containment time ~10% is obtained.

In these computer experiments, some of instabilities have been inhibited, and the effective collision time has been restricted by computer time to the value which has been only a few times greater than the mean transit time of ions. This situation has probably caused favorable results in the improvement in the energy confinement by the applied rf electric field. For instance, the absence of instabilities which may be associated with the rf electric field does not give anomalous losses, and a number of collisions may restraine ions from beeing separated into two groups by the rf electric field.

Acknowledgements

The authors wish to express their sincere thanks to Profs. K. Takayama, Y. Terashima, R. Itatani and H. Nishihara for their discussions and encouragements. They also thank to Prof. H. Obayashi for his useful suggestions. They owe to Mrs. T. Yamada and K. Kawai for their original computation code. This work has been carried out under the Collaborating Research Program at the Institute of Plasma Physics, Nagoya University.

Appendix A Classical mirror loss

The classical mirror loss is caused by Coulomb collisions which change the pitch angle $\theta = \tan^{-1}(v_\perp/v_\parallel)$ of an ion. In order to obtain the particle containment time τ_n, we determine the distribution function f for ions. For simplicity, we introduce sources which provide new particles and are distributed uniformly throughout the entire volume, and analyze the stationary problem. For purposes of further simplification, we assume that the magnetic field is uniform over the entire volume, and that it rises rapidly at the ends. Then, the kinetic equations in the trapped region (I) and in the loss cone (II) can be written, respectively:

$$-\left(\frac{\partial f_I}{\partial t}\right)_c = q \qquad \text{for } \pi - \theta_0 > \theta > \theta_0 \tag{A1}$$

$$-\left(\frac{\partial f_{II}}{\partial t}\right)_c = q - \ell \quad \text{for } \theta_0 > \theta > 0, \pi - \theta_0 > \theta > \theta_0 \ , \tag{A2}$$

where $\theta_0 = \sin^{-1}\sqrt{1/R_m}$ is the loss angle, and $(\partial f/\partial t)_c$ denotes the change of the distribution function by means of collisions. The source density q and the loss density ℓ are assumed independent of θ , and the relation $\int q \, d\vec{v} = \int \ell \, d\vec{v}$ should hold. We assume also that the containment time for ions in the loss cone is nearly equal to the mean transit time $\langle \tau_{it} \rangle$.

Since we are seeking the distribution function in the form

$$f = F(\theta) \quad \exp(-Mv^2/2T), \tag{A3}$$

we rewrite Eqs.(A1) and (A2):

$$-\frac{A_D}{v^3}\frac{2x^2\Phi(x)-\Phi(x)+x\Phi'(x)}{2x^2}\frac{1}{\sin\theta}\frac{\partial}{\partial\theta}\sin\theta\frac{\partial f}{\partial\theta}\begin{cases}=q & \text{in the trapped region,}\\ =q-\ell & \text{in the loss cone,}\end{cases} \tag{A4}$$

where x stands for $v\sqrt{M/2T}$. The quantity A_D is the diffusion constant[12] and $\Phi(x)$ is the error function.

As is easily seen the boundary conditions are given by

$$\partial f_I/\partial\theta = 0 \qquad \text{for } \theta = \pi/2 \ ,$$

$$\partial f_{II}/\partial\theta = 0 \qquad \text{for } \theta = 0, \ \pi \ ,$$

$$f_I = f_{II} \qquad \text{for } \theta = \theta_0 \ , \ \pi - \theta_0 \ ,$$

and

$$\frac{\partial f_I}{\partial\theta} = \frac{\partial f_{II}}{\partial\theta} \qquad \text{for } \theta = \theta_0 \ , \ \pi - \theta_0 \ . \tag{A5}$$

Through straightforward calculations, we obtain the particle containment time, $\tau_n \equiv \int (f_I + f_{II})d\vec{v}/\int \ell \ d\vec{v}$, approximately in the form

$$\tau_n \simeq \tau_{ic} \ln R_m + 2R_m \langle\tau_{it}\rangle \ , \tag{A6}$$

where the collision time τ_{ic} is given by

$$\tau_{ic} = \frac{1}{(2\pi T/M)^{3/2}}\int\frac{A_D}{v^3}\frac{2x^2\Phi(x)-\Phi(x)+x\Phi'(x)}{2x^2}\exp(-\frac{Mv^2}{2T})d\vec{v} \ . \tag{A7}$$

In the usual condition, the second term on the rhs of Eq.(A6) can be neglected, while this term is important in our simulation.

Appendix B Banana orbit

As is well known[13], the cross field diffusion is enhanced by the "banana" orbit of a charged particle in Tokamaks, as compared with the classical one. A similar phenomenon can be observed also in a toroidal quadrupole.

In the absence of collisions, the total angular momentum P_ψ of a charged particle is conserved in the toroidal quadrupole:

$$P_\psi = M(R + x)v_\psi + e(R + x)A_\psi \equiv \text{const}, \qquad \text{(B1)}$$

where A_ψ, the component of the vector potential along the toroidal axis, is given by

$$A_\psi = \frac{1}{2} aB_c\left[\left\{1 - \frac{1}{3}\varepsilon\frac{x}{a}\right\}\frac{x^2}{a^2} - \frac{y^2}{a^2}\right] . \qquad \text{(B2)}$$

We consider that the aspect ratio $\varepsilon^{-1} \equiv R/a$ is much larger than unity and that the nonadiabatic nature can be neglected. Then we easily find two types of the trajectory, i.e., one is banana-like and the other four-cusped. This difference is due to the initial condition: the position $(x_1, 0)$ and the sign of v_ψ. The velocity v_ψ is approximated in the form

$$v_\psi = \pm \frac{B_t}{B}\left\{\frac{2}{M}(E - \mu B)\right\}^{1/2}, \qquad \text{(B3)}$$

where both the energy E and the magnetic moment μ are constant.

Introducing the "banana" size δr on the X axis, we rewrite Eq.(B1) as for the "banana" orbit:

$$P_{\psi}(x_1) = P_{\psi}(x_1 + \delta_r). \qquad \text{(B4)}$$

Then a substitution of Eqs.(B2) and (B3) into Eq.(B4) gives an approximate relation

$$\frac{\delta r^2}{a^2} + 2\,\frac{x_1}{a}\,\frac{\delta r}{a} - \frac{4\gamma\{\gamma^2 + (x_1/a)^2\}^{-1/2} - 2\{\mu B_t/E\}}{\{a/r_L\} + \gamma\{\gamma^2+(x_1/a)^2\}^{-3/2}} = 0\ , \qquad \text{(B5)}$$

where r_L is defined by $\sqrt{2ME}/eB_c$. Consequently, the "banana" size is comparatively large at the central region and is approximated as

$$\delta r \simeq \sqrt{2}\ r_L\ \sqrt{a/r} \qquad \text{for} \qquad r_L << \gamma^2 a$$

and $\qquad \text{(B6)}$

$$\delta r \simeq \sqrt{2}\ \gamma a \qquad \text{for} \qquad r_L >> \gamma^2 a \quad .$$

REFERENCES

1) C.J.H. Watson and L.G. Kuo-Petravic,
Phys. Rev. Let. 20, 1231 (1968).

2) S. Miyake, T. Sato, K. Takayama, T. Watari, S. Hiroe,
T. Watanabe and K. Husimi,
J. Phys. Soc. Japan 31, 265 (1971).

3) A.J. Hatch and J.L. Shohet,
Phys. Fluids 17, 232 (1974).

4) H. Abe, K. Kawai, T. Yamada and R. Itatani,
J. Phys. Soc. Japan 33, 216 (1972).

5) J.E. Howard, Phys. Fluids 13, 2407 (1970).

6) W.H. Hooke, M.A. Rothman, J. Sinnis and J. Adam,
Phys. Fluids 8, 1146 (1965).

7) A.J. Lichtenberg and G. Melin,
Phys. Fluids 16, 1660 (1973).

8) C.J.H. Watson, EUR-CEA-FC-628-AG, 67 (1971).

9) O. De Barbieri, EUR-CEA-FC-628-AG, 75 (1971).

10) T. Kawamura, H. Momota, C. Namba and Y. Terashima,
Nucl. Fusion 11, 339 (1971).

11) D.J. BenDaniel, J. Nucl. Energy, Pt. C 3 235 (1961).

12) L. Spitzer, Jr., "Physics of Fully Ionized Gases",
(Interscience Publishers, Inc., New York, 1956) p.129.

13) A.A. Galeev and R.Z. Sagdeev,
Sov. Phys. JETP 26, 233 (1968).

Table I Physical quantitites for simulations

B_c	= 5000 Gauss
B_t	= 2500, 1450, and 500 Gauss respectively
a	= 0.25 m
M	= 1.67×10^{-27} kg
$T_{i\cdot initial}$	= 300 eV (Maxwellian)
τ_{ic}	= 12 μsec

Table II Ions lost into rf electrondes

R_m	N_1/N_2	$\langle W_1 \rangle$	$\langle W_0 \rangle$
3	~ 6 %	~ 5 keV	~ 500 eV
5	~ 3 %	~ 5 keV	~ 500 eV
14	0	——	~ 500 eV

N_1 : Number of ions lost into rf electrodes,

N_2 : Total number of lost ions,

$\langle W_1 \rangle$: Mean energy of ions lost into rf electrodes,

$\langle W_0 \rangle$: Mean energy of contained ions.

Table III Parameters of the system and physical quantities

(a)	B_{max}	= 11250 Gauss
	B_{min}	= 3750 Gauss
	R	= 2.5 m
	a	= 0.25 m
	C	= 1.5×10^{5} $(V/m)^2/eV$
	ω_r	= 6.8×10^{7} rad/sec
(b)	M	= 1.67×10^{-27} kg
	$T_{i\cdot ini}$	= $T_{e\cdot ini}$ = 300 eV (Maxwellian)
	initial density	= 1.6×10^{14} m^{-3}
	τ_{ic}	= 12 μ sec

Table IV Quantities for the computation

line density of super particles	= 1.7×10^{9} m^{-1}
mass ratio of an ion to an electron	= 25
initial number of super ions and electrons	= 1500 respectively

FIGURE CAPTIONS

Fig.1 Schematic cross section of the toroidal quadrupole and principal coordinates of the system.

Fig.2 Adiabatic parameter A vs distance from the cneter $\sqrt{x^2 + y^2}$, along the line $y = x$ or $y = -x$ in the toroidal quadrupole.

Fig.3 Trajectory of an ion (a) and time variation of μ (b) for the case of $A_i|_{min} \simeq 1.5$. The magnetic moment varies after the passage through the nonadiabatic region, and the ion escapes finally to an open end.

Fig.4 Time variation of μ without collisions for the case of $A_i|_{min} \simeq 8$ (a). The magnetic moment recovers the previous value after the passage through the nonadiabatic region. On the contrary, the change of the magnetic moment is enhanced by rare collisions (b).

Fig.5 Decay curves of the particle number for the cases of $R_m = 3$ (dashed curve), $R_m = 5$ (chained curve), and $R_m = 14$ (solid curve).

Fig.6 Schematic "banana" orbit of the guiding center of a charged particle in the toroidal quadrupole. A dashed curve denotes a line of force, and δr is the "banana" size.

Fig.7 Evolution of the mean ion energy. Applied rf electric fields E_0 are *20* kV/m (Curve I), *10* kV/m (Curve II), and *5* kV/m (Curve III), respectively. Dashed lines indicate the change by means of Eq.(3.2), where coefficients α are respectively *0.75* (Curve I), *0.85* (Curve II), and *0.8* (Curve III) $eV \cdot sec^{-1} \cdot (V/m)^{-2}$.

Fig.8 Decay of the particle number, and evolutions of the contained ion energy and the lost ion energy, for the case of $E_0 = 20$ kV/m. The loss rate is gradually increased when the ion energy is increased and condition (3.4) breaks down.

Fig.9 Improvement in the energy containment time τ_E by means of the feedback control of the applied rf electric field. The quantity C is defined by the ratio $E_0^2/\langle W_i \rangle$.

Fig.10 Comparison of the result for the case of $C = 1.5 \times 10^5$ $(V/m)^2/eV$ (solid curves) with that for the case of no rf electric field (dashed curves). The decay of the particle number and evolutions of the contained ion energy and the lost ion energy are demonstrated. The applied rf electric field is turned on at the time $t = 3$ μsec.

Fig.11 Increase of the mean ion energy for the case $C = 2.5 \times 10^5$ $(V/m)^2/eV$. The applied rf electric field is turned on at the time $t = 3$ μsec. Dashed curve corresponds to that with the heating rate $\tau_H^{-1} = 1.4 \times 10^5$ sec^{-1}.

Fig.12 Decay curves of ions and electrons. In Experiment I (solid curve), the rf electric field is applied from the time $t = 3$ μsec till the time $t = 18$ μsec. In Experiment II (dashed curve), no rf electric field is applied, and in Experiment III (chained curve), the rf electric field is turned off at the time $t = 12$ μsec.

Fig.13 Distributions of the plasma potential in Experiment II (a) and in Experiment I (b) at the time $t = 9$ μsec. The outer square is the wall of the container, and the equipotential curves are drawn at intervals of 20 volt.

Fig.14 Evolutions of the contained plasma energy and the lost plasma energy.

Fig.15 Time variations of the mean ion energy (a) and the mean electron energy (b).

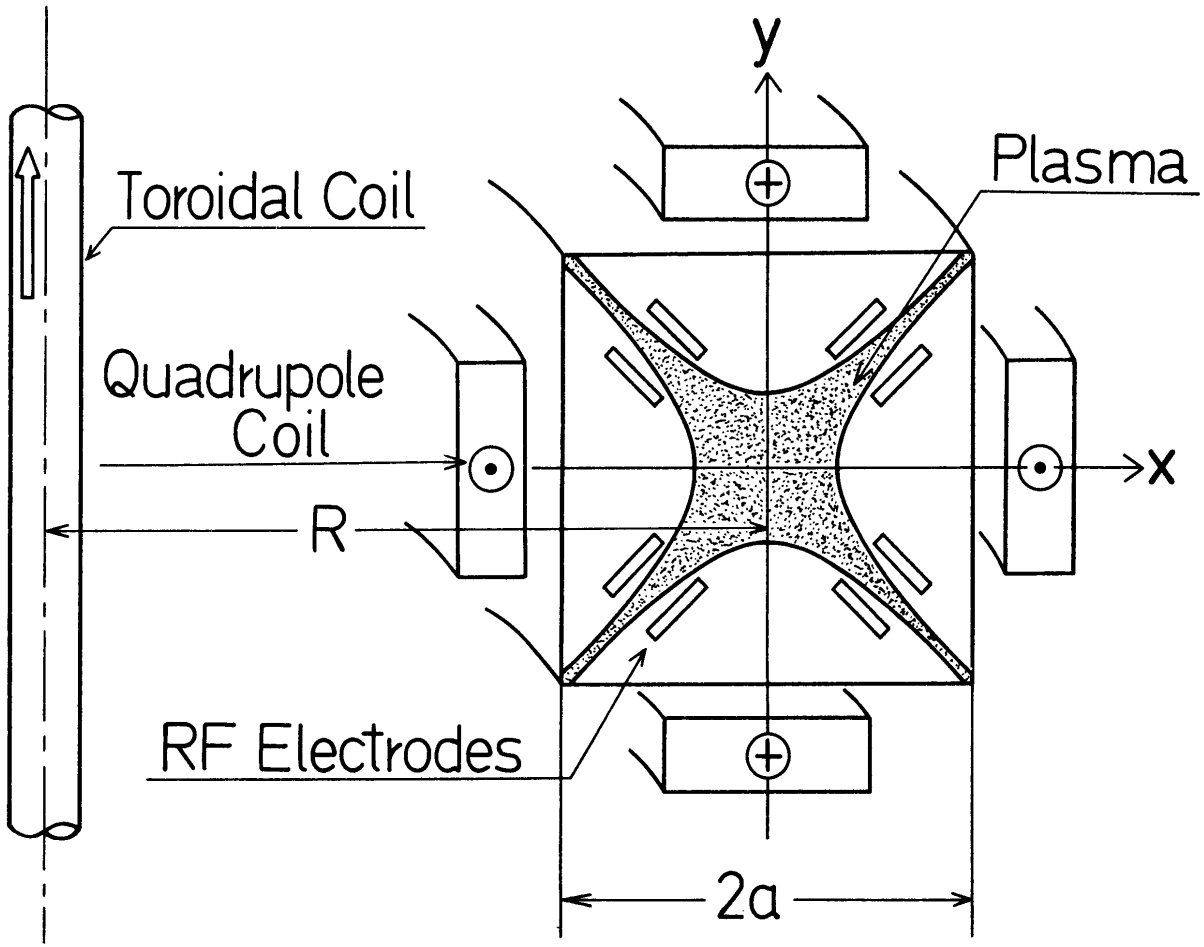

Fig. 1

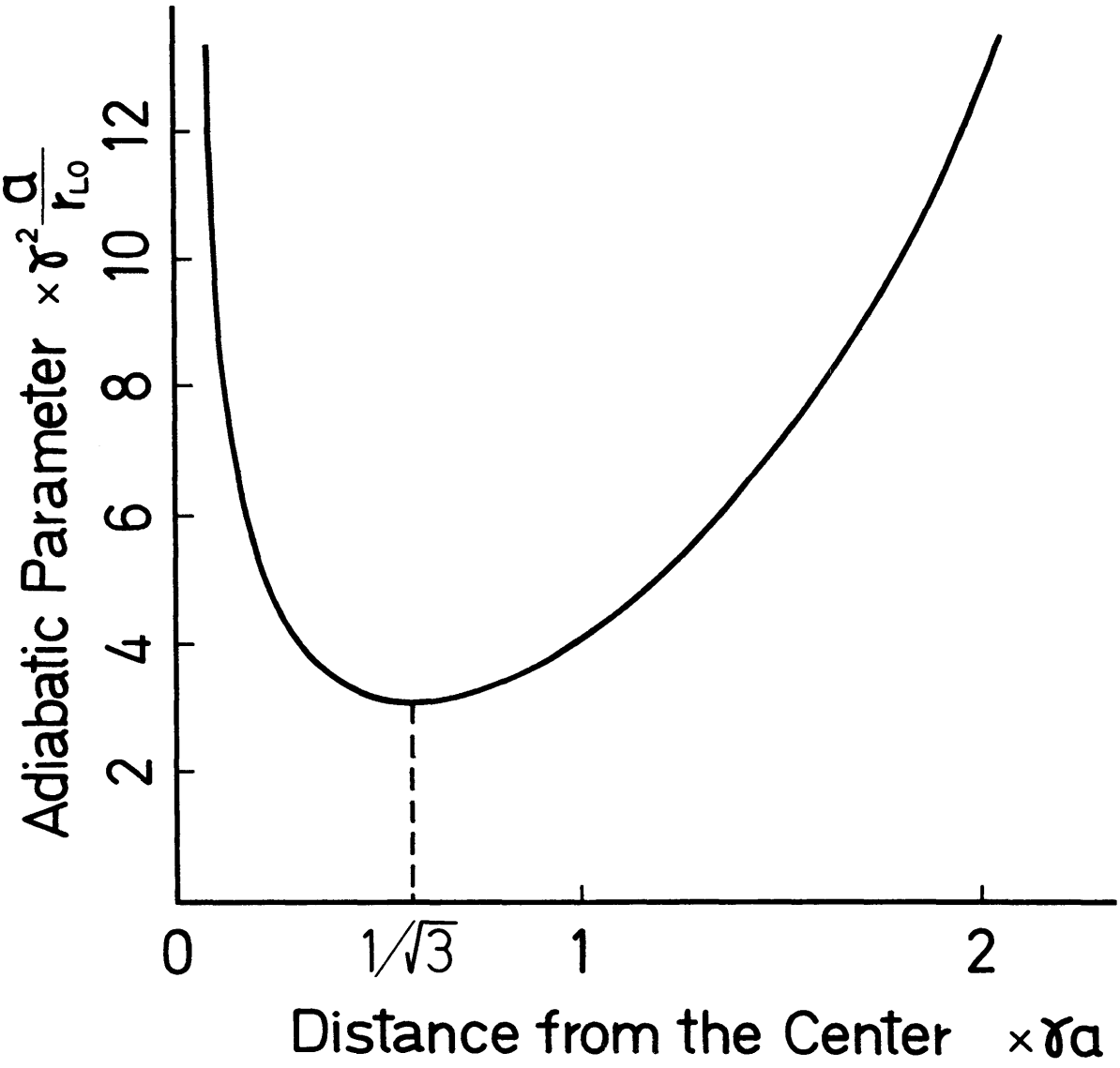
Adiabatic Parameter $\times \gamma^2 \frac{a}{r_{L0}}$
2
4
6
8
10
12
0
$1/\sqrt{3}$
1
2
Distance from the Center $\times \gamma a$

Fig. 2

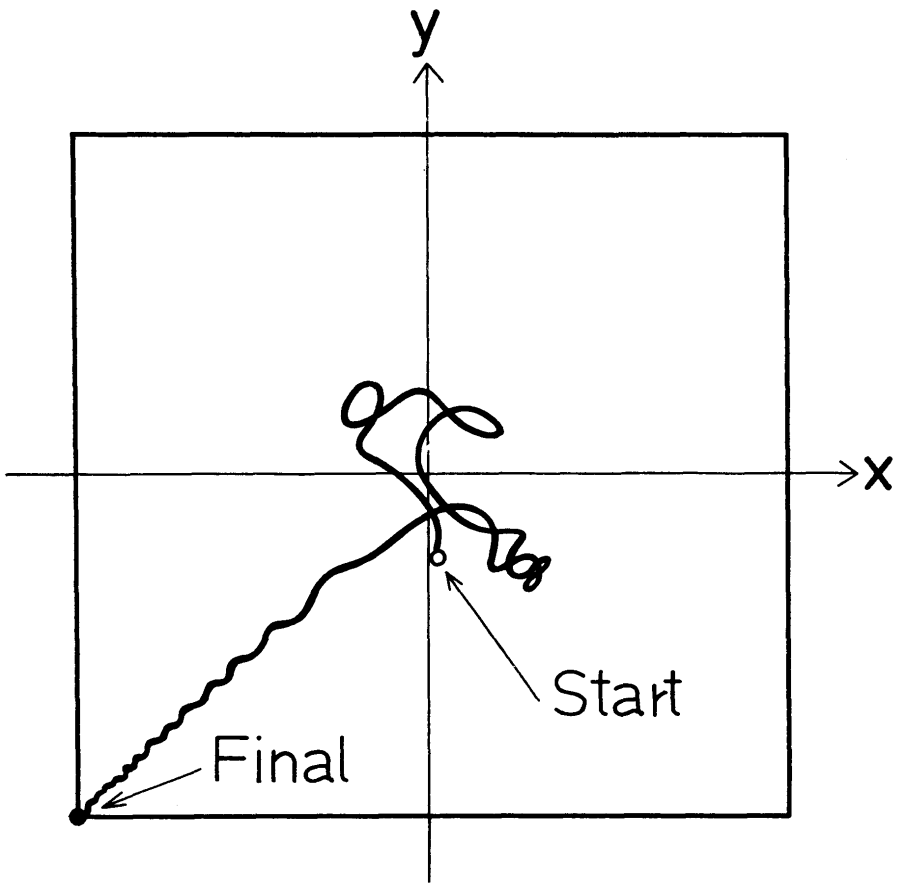

Fig. 3 (a)

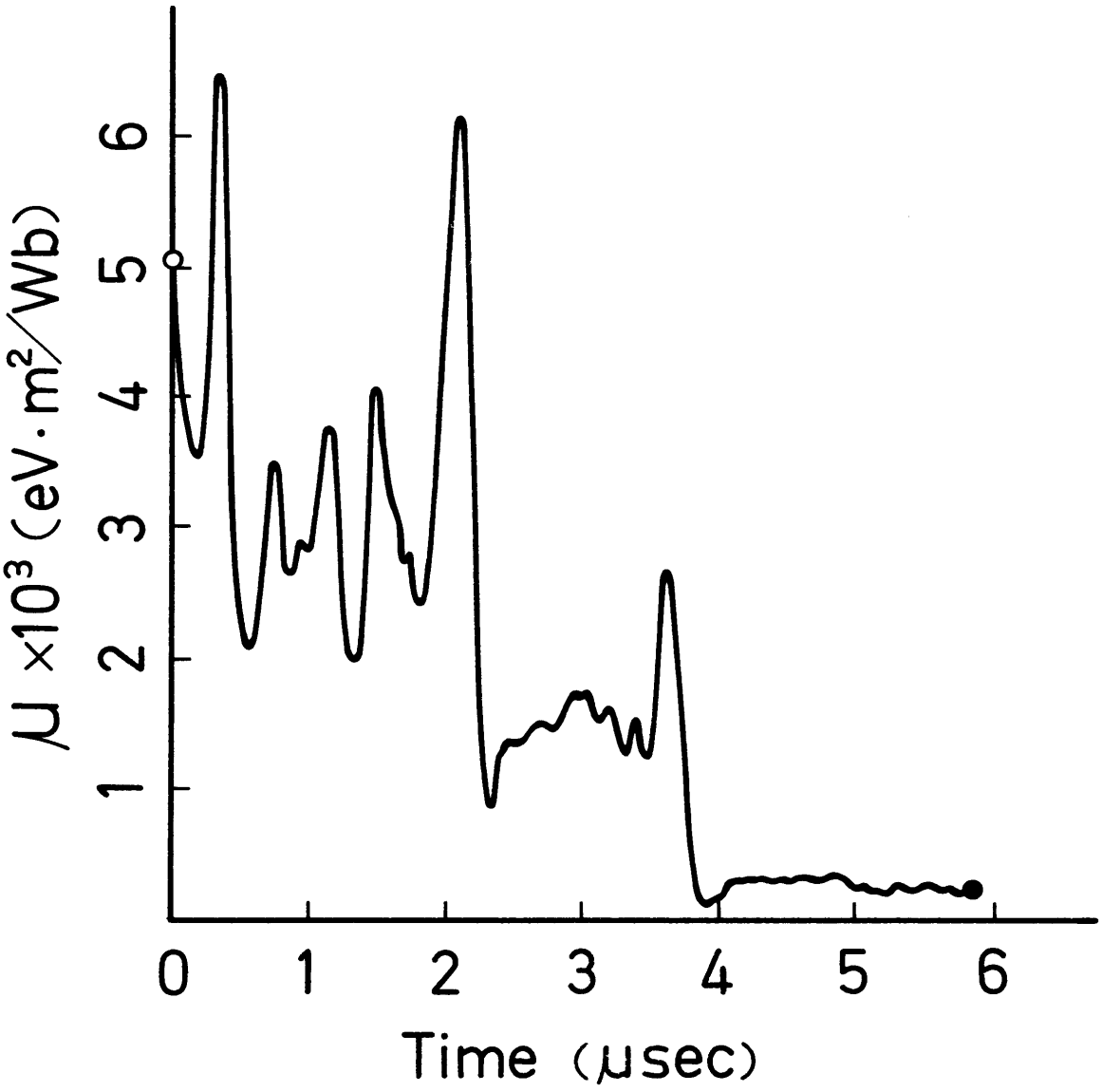

Fig. 3 (b)

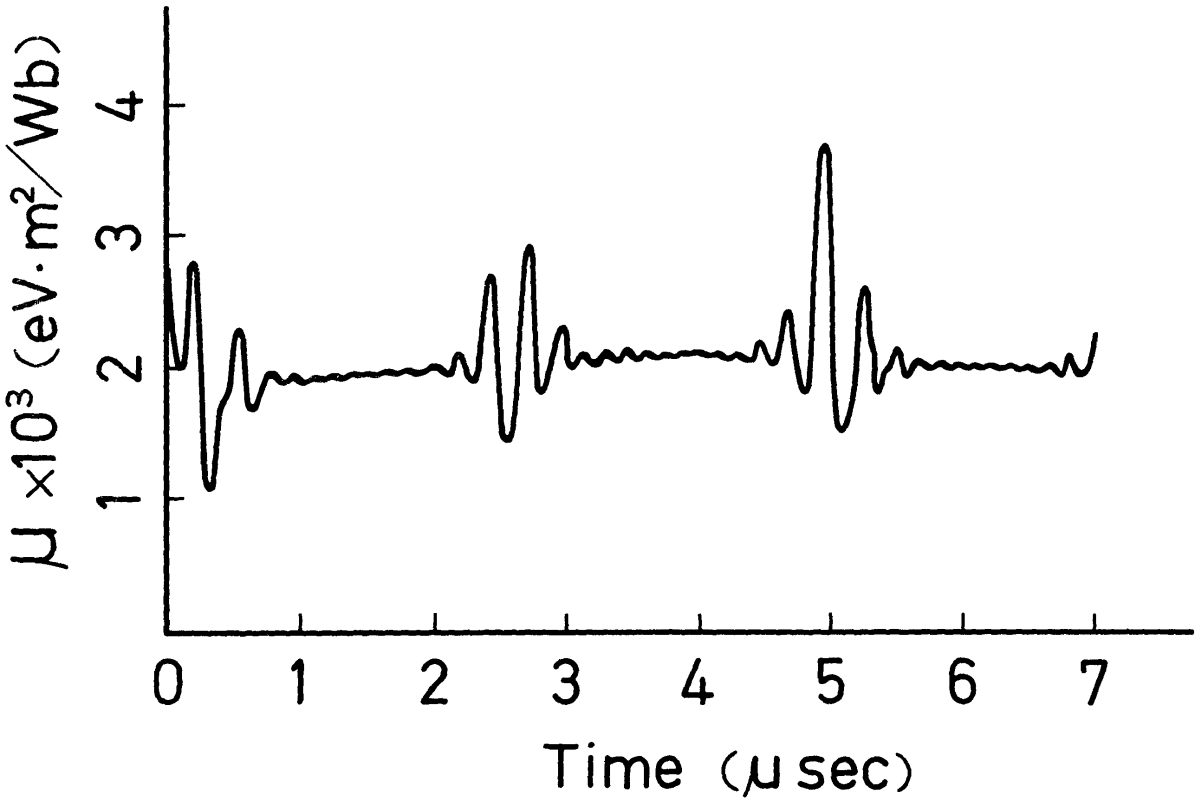

Fig. 4 (a)

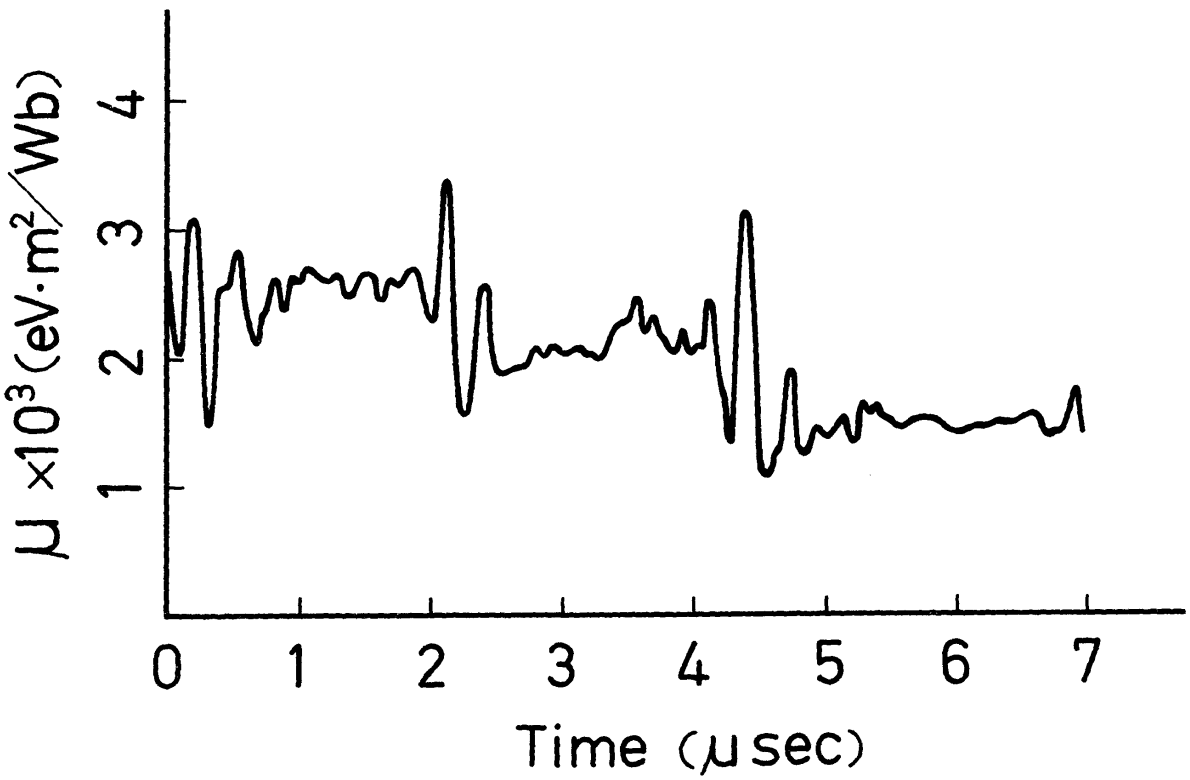

Fig. 4 (b)

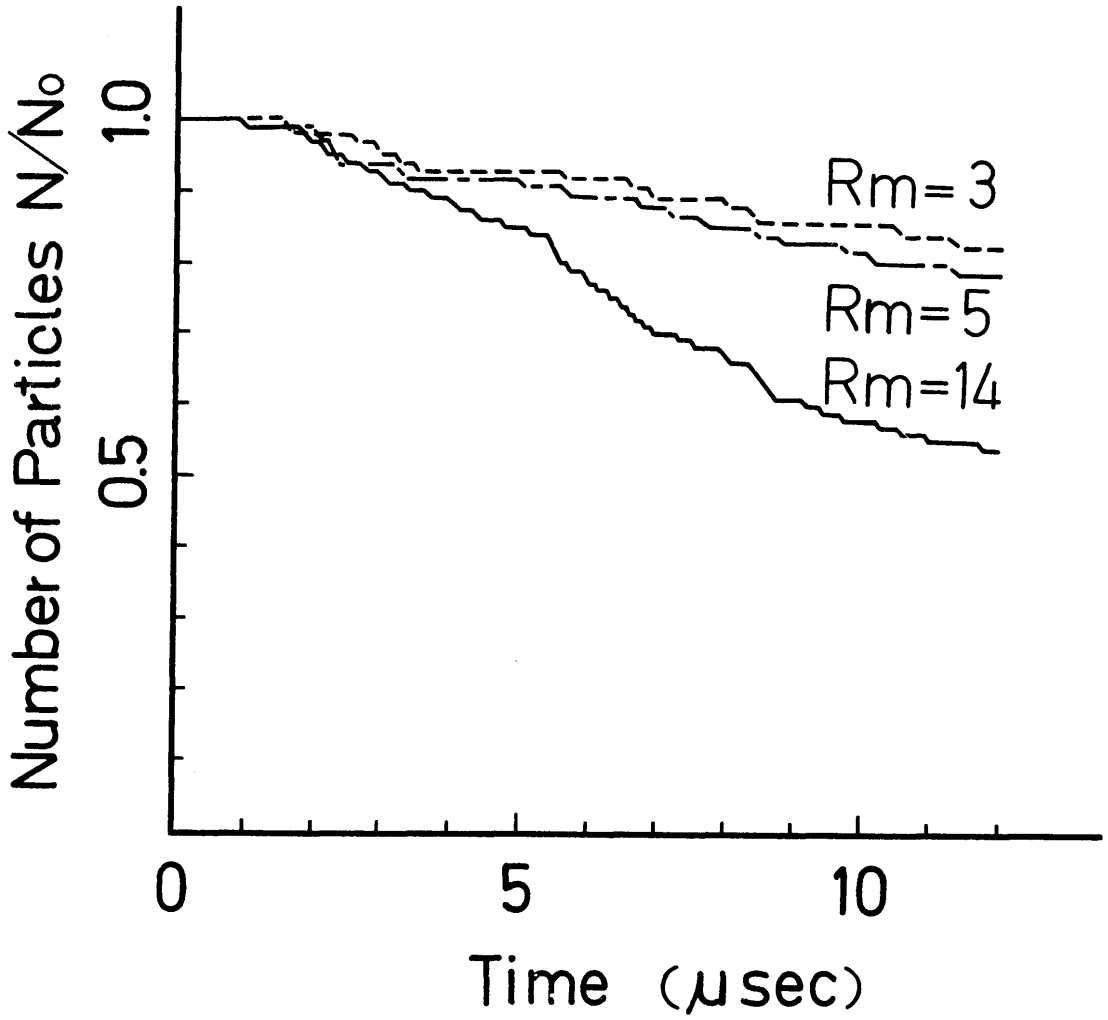

Fig. 5

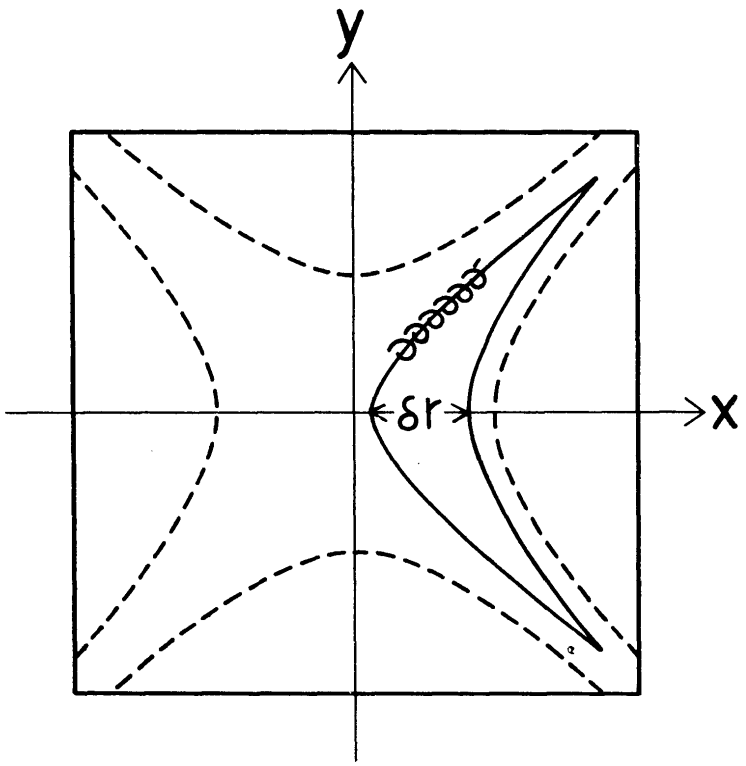

Fig. 6

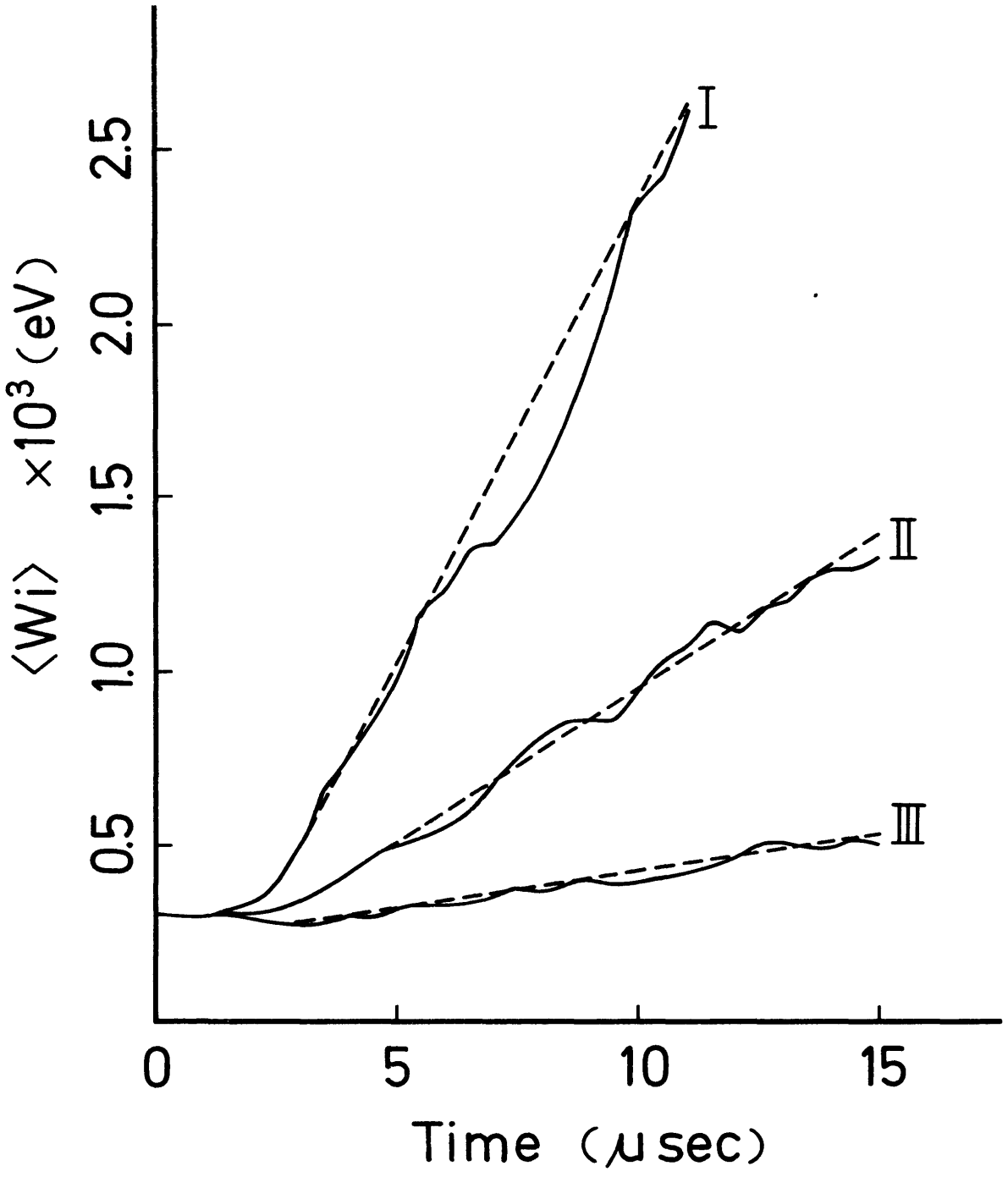

Fig. 7

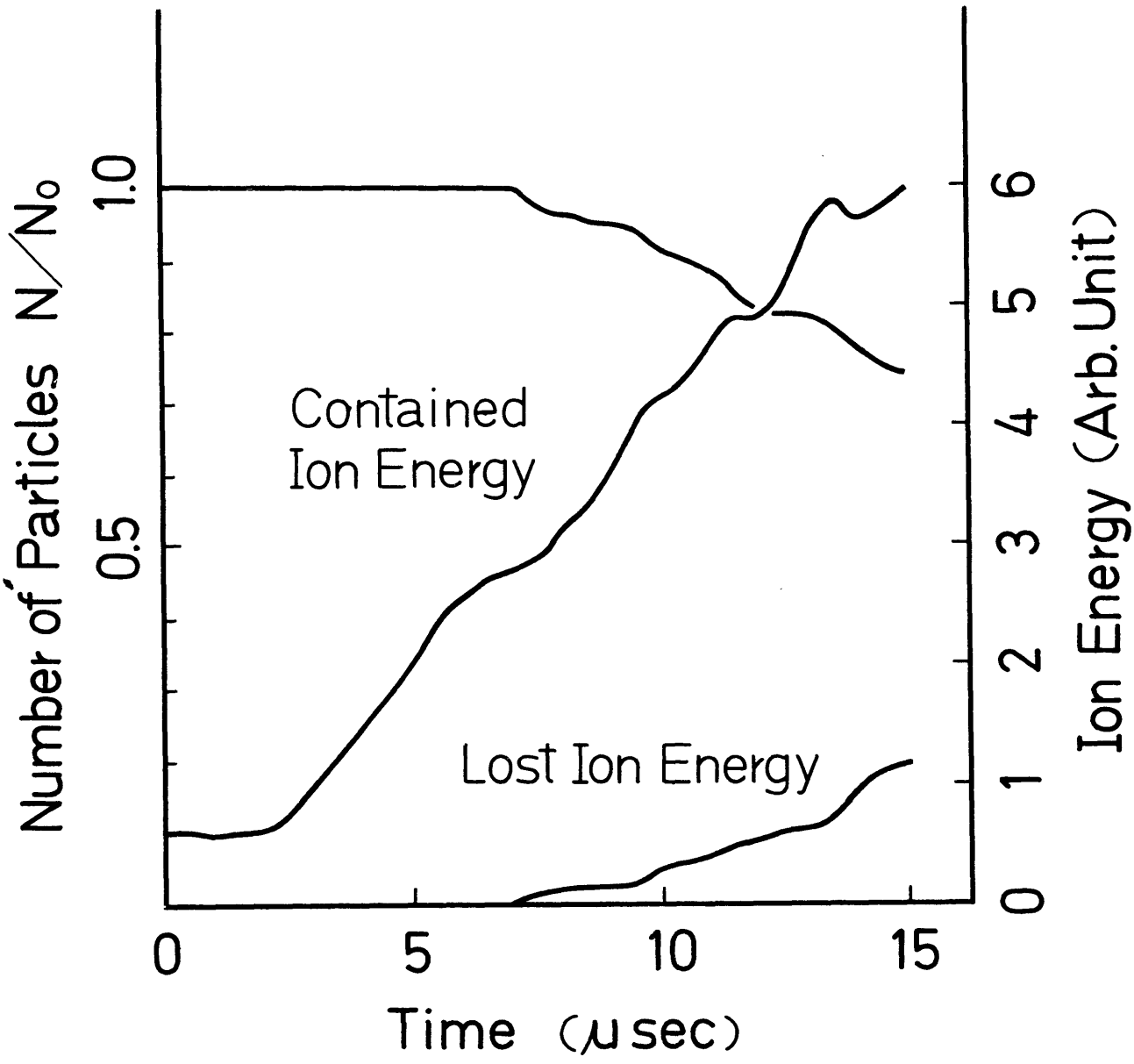
Number of Particles N/N₀
1.0
0.5
Contained
Ion Energy
Lost Ion Energy
0
5
10
15
Time (μsec)
0
1
2
3
4
5
6
Ion Energy (Arb. Unit)

Fig. 8

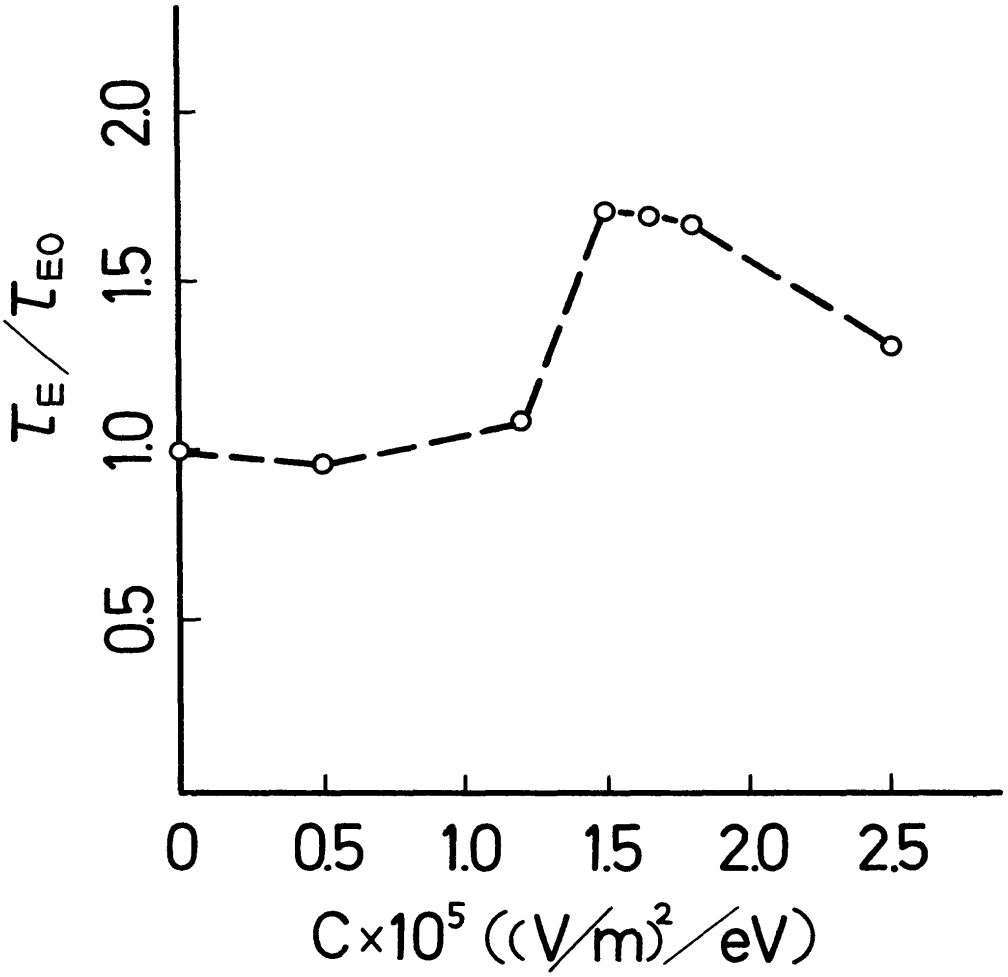

Fig. 9

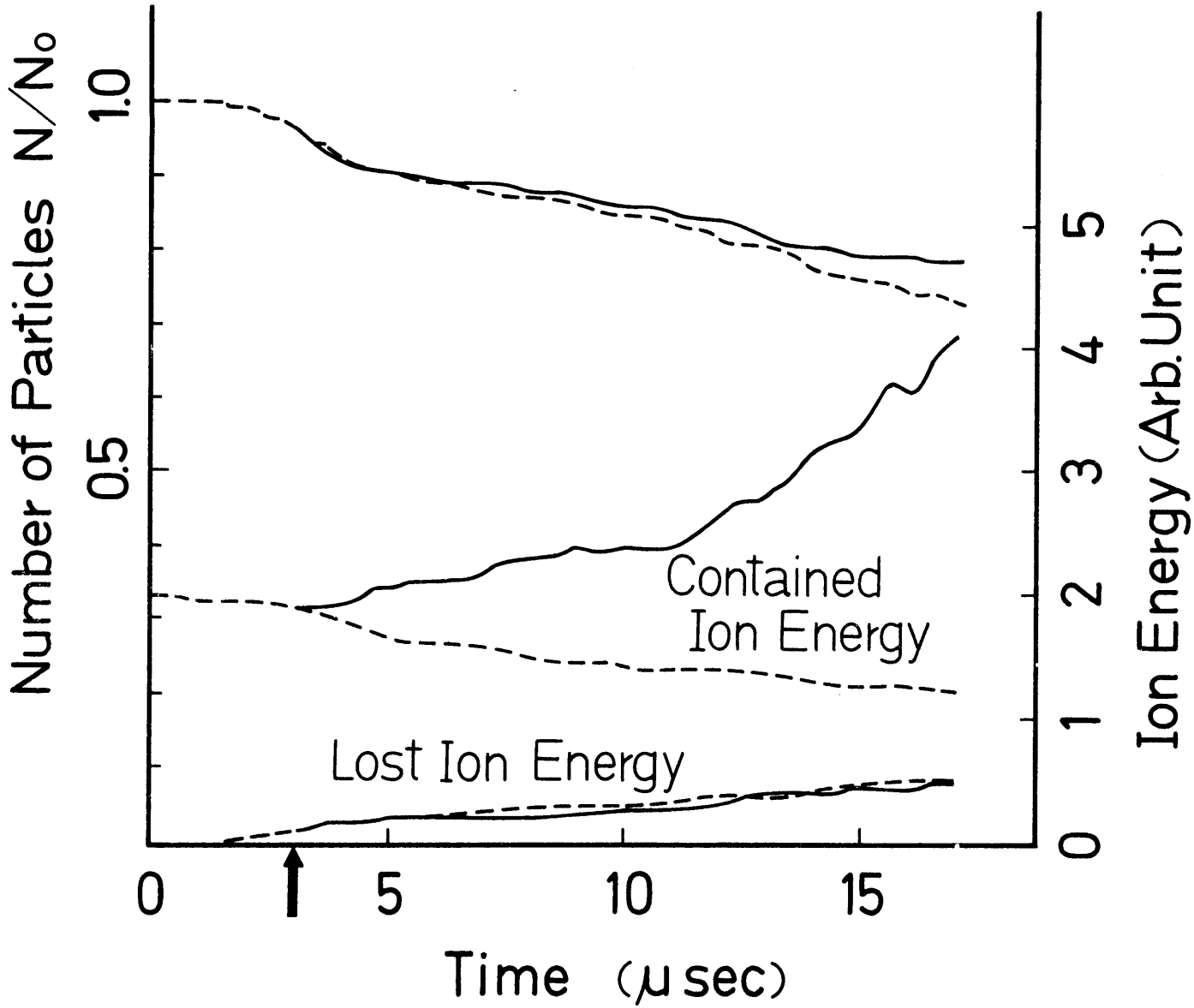
Number of Particles N/N₀
1.0
0.5
0
5
10
15
Time (μsec)
Contained
Ion Energy
Lost Ion Energy
0
1
2
3
4
5
Ion Energy (Arb.Unit)

Fig. 10

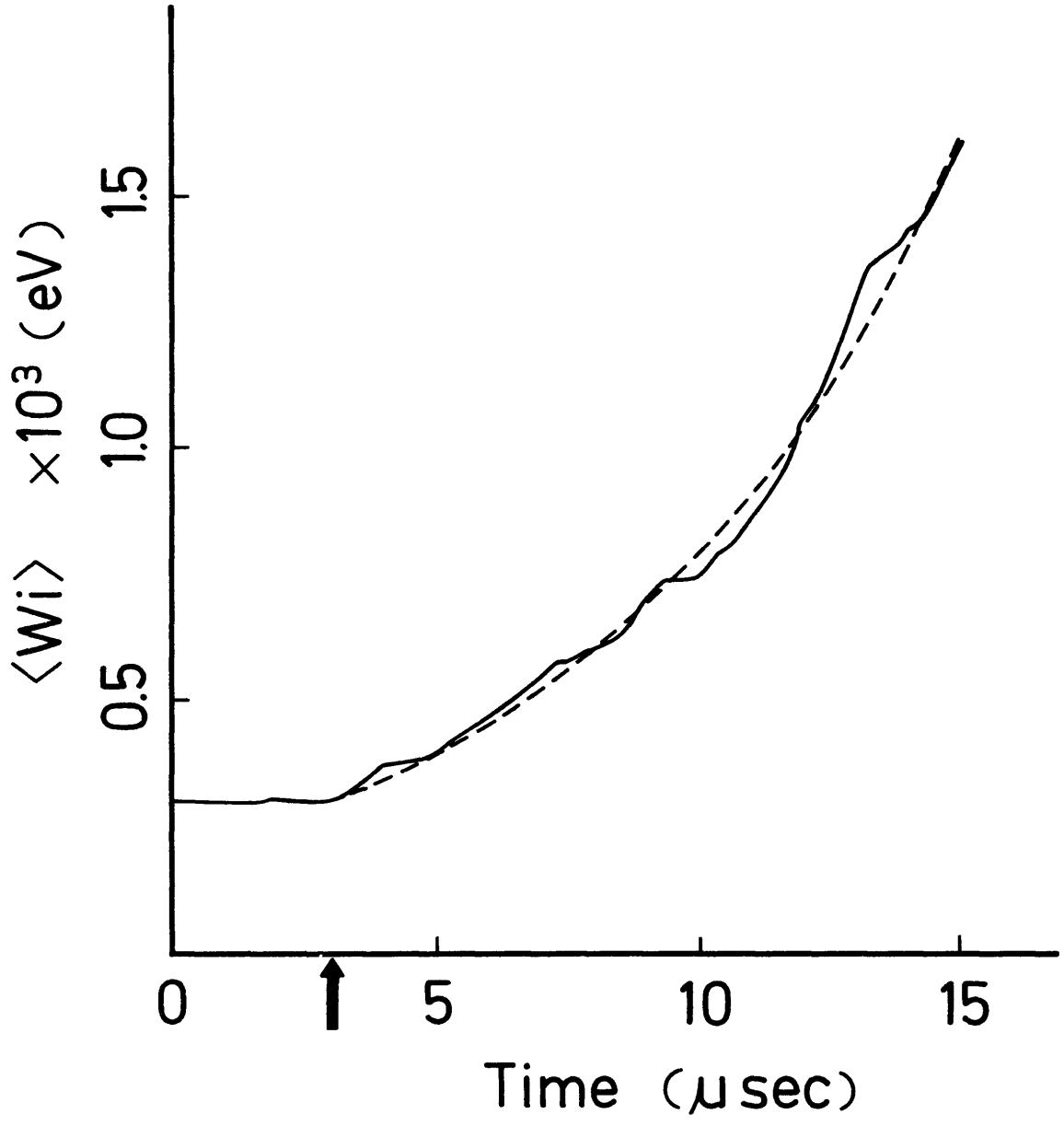

Fig. 11

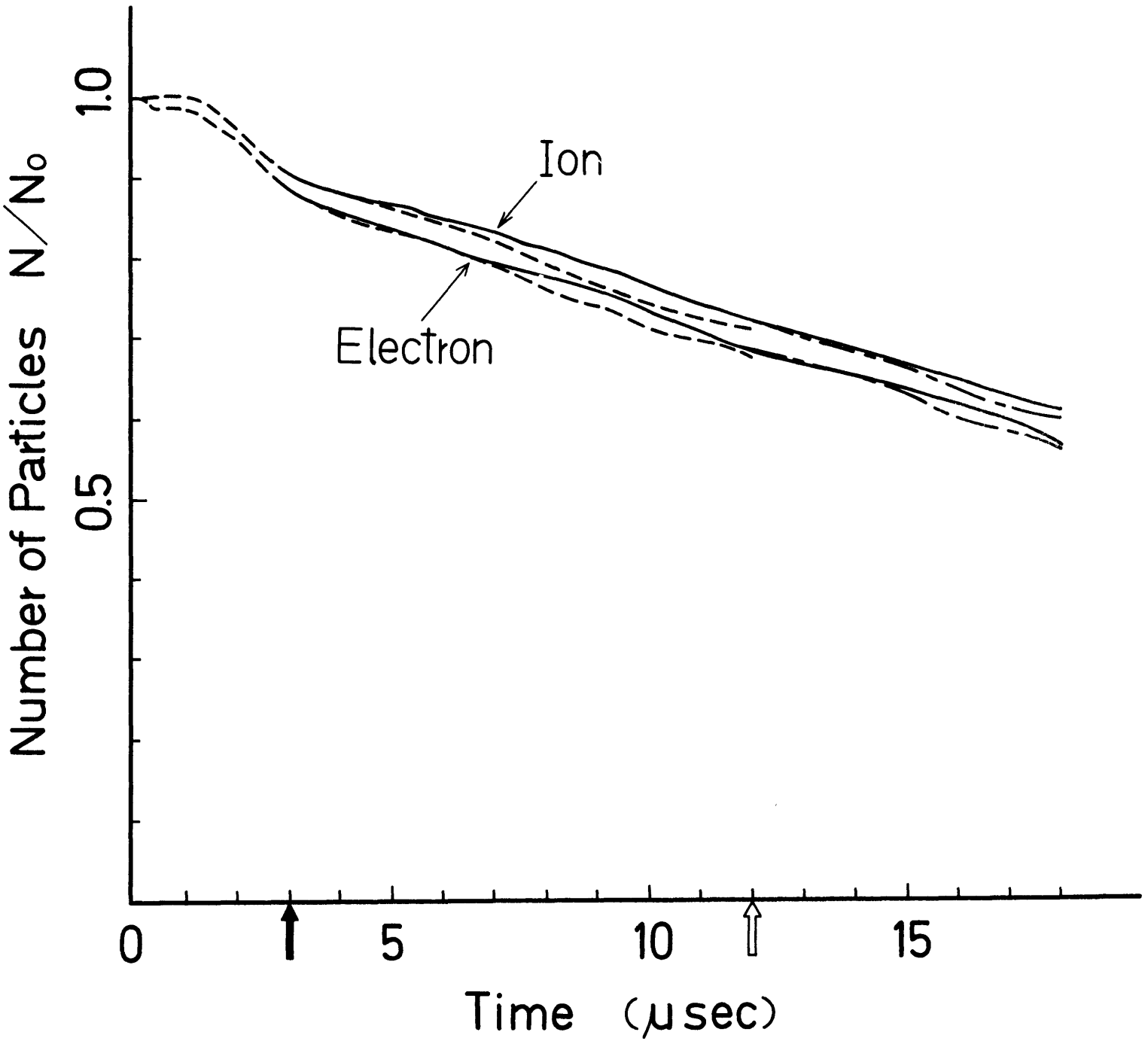

Fig. 12

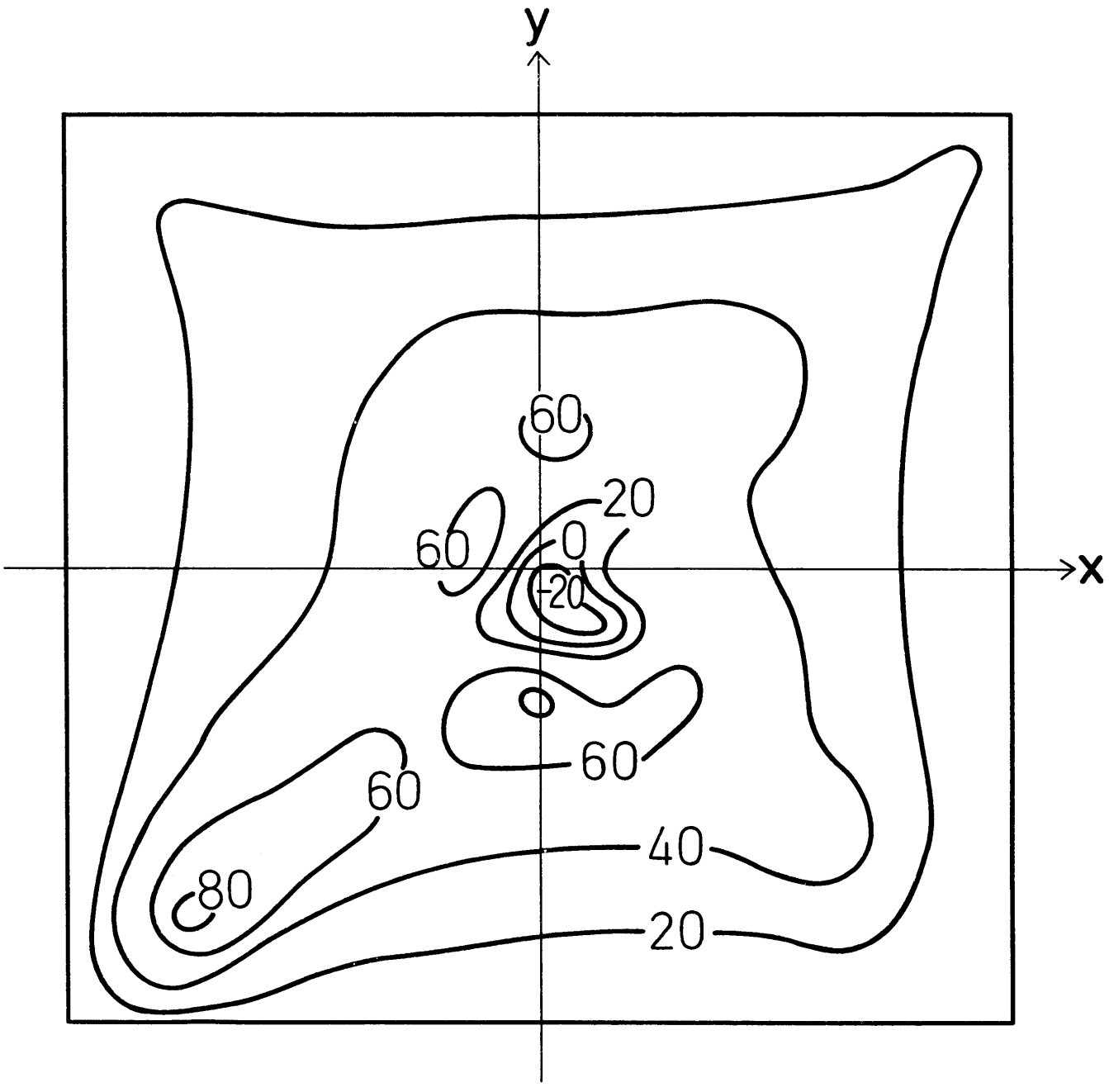

Fig. 13 (a)

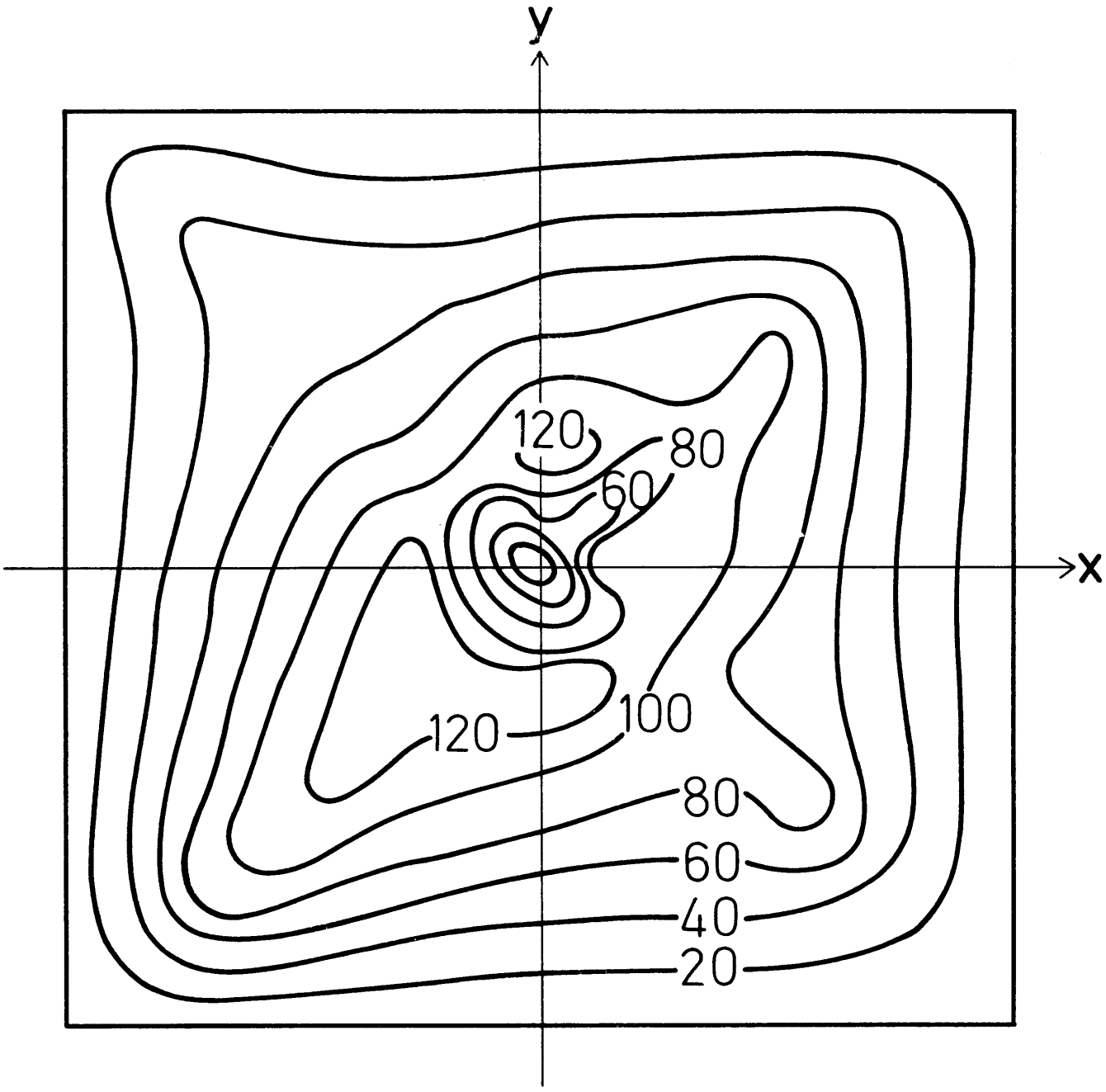

Fig. 13 (b)

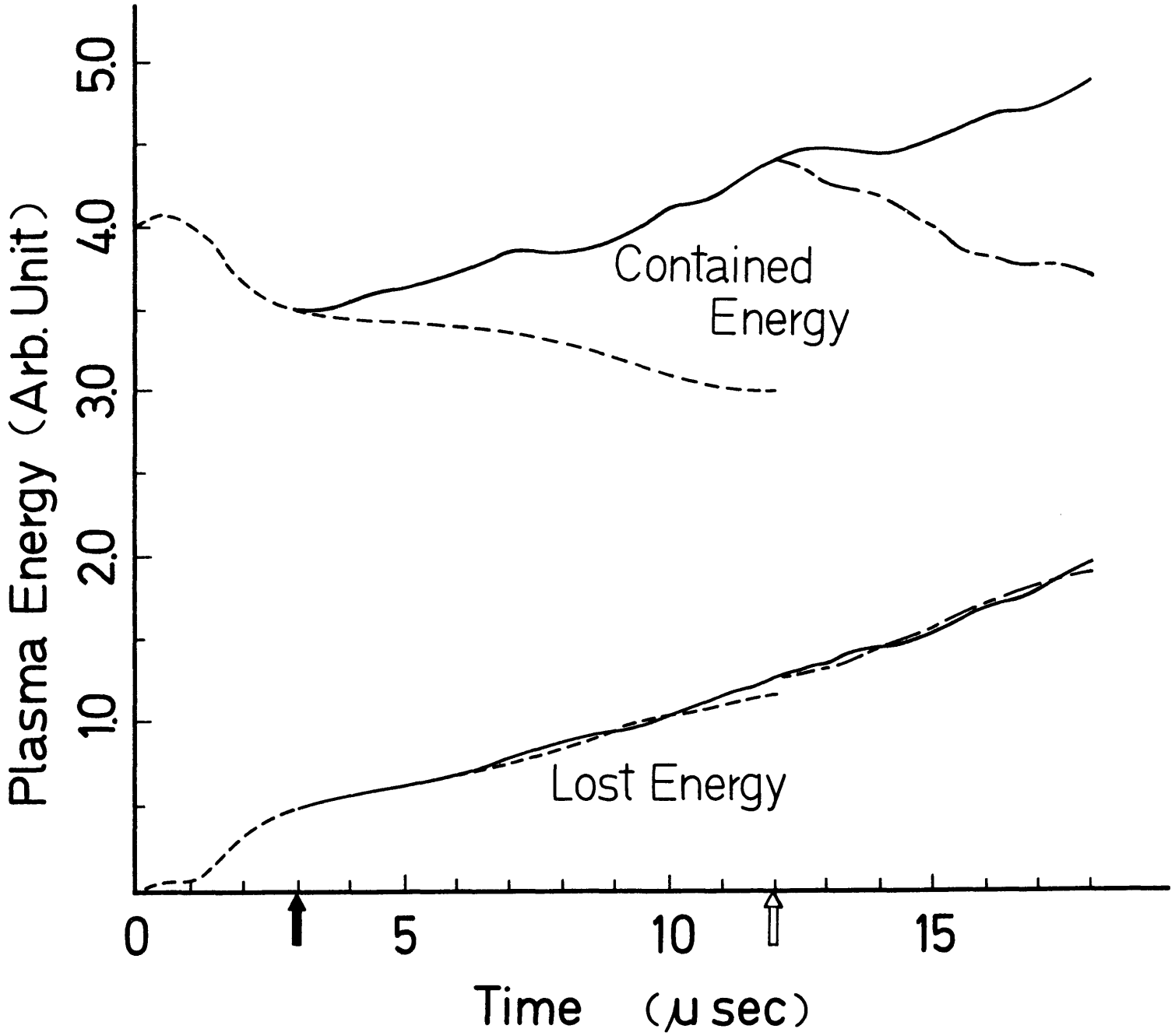
Plasma Energy (Arb. Unit)
1.0
2.0
3.0
4.0
5.0
Contained Energy
Lost Energy
0
5
10
15
Time (μ sec)

Fig. 14

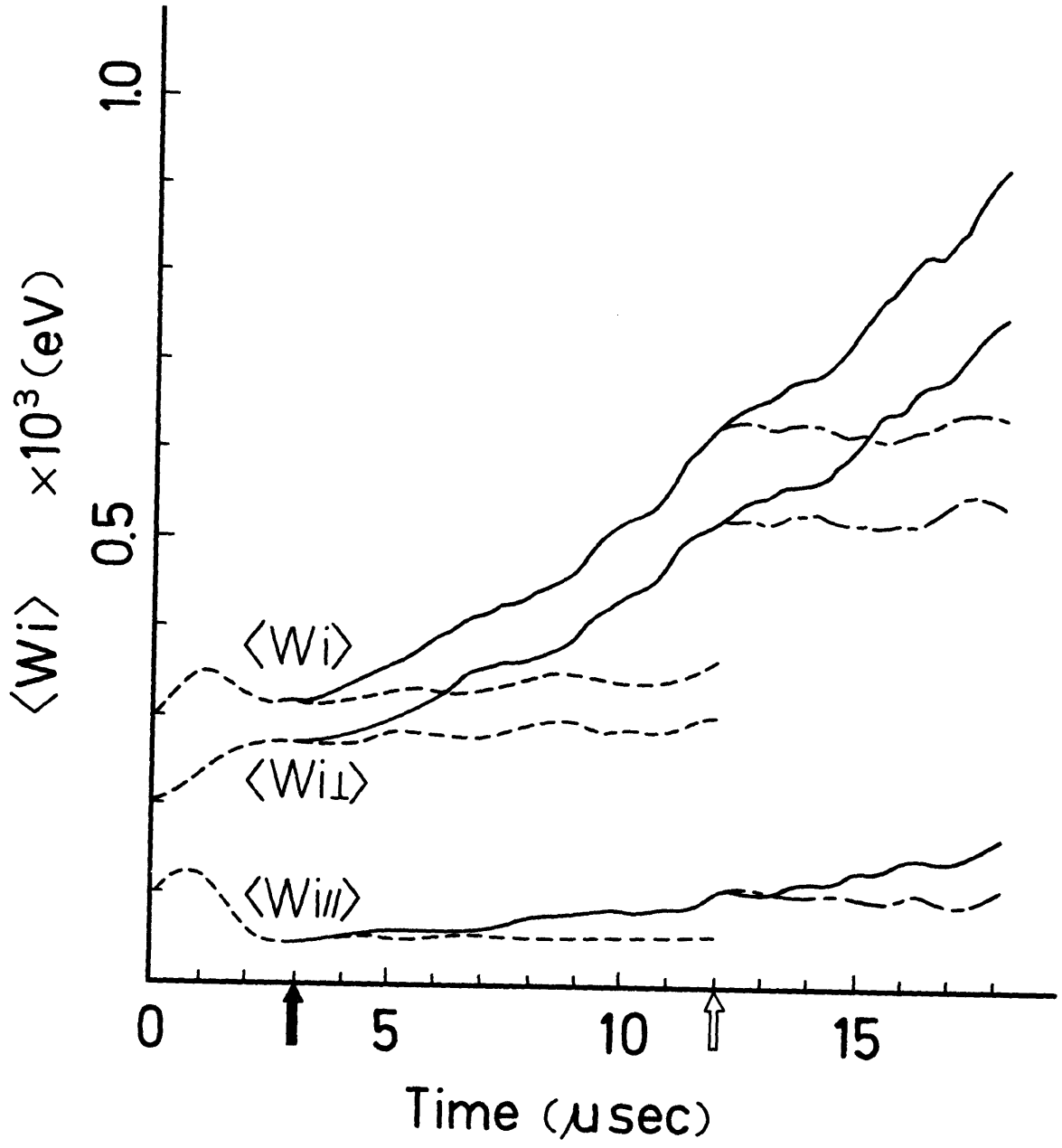

Fig. 15 (a)

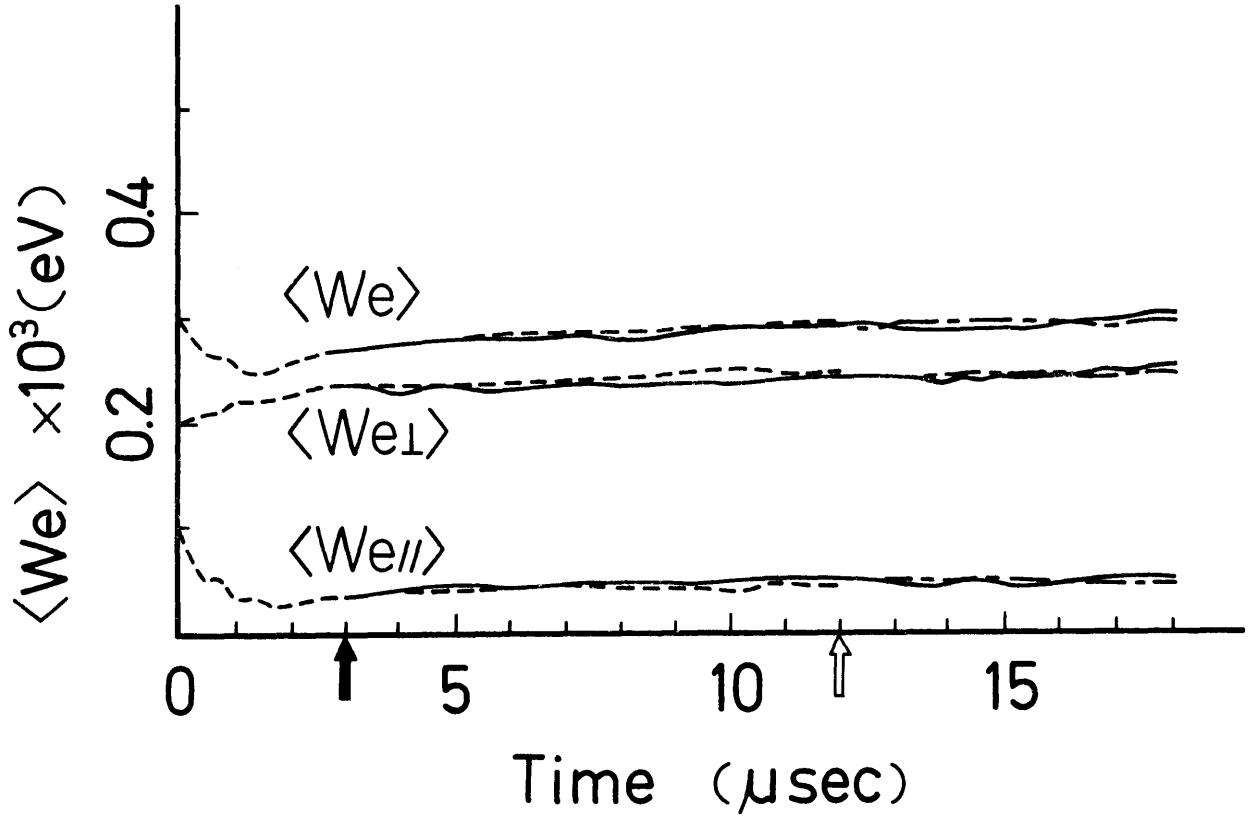

Fig. 15 (b)